Temperature effects on DLC coated micro moulds

C.A. Griffiths, A. Rees, R.M. Kerton, O.V. Fonseca

PII: S0257-8972(16)30777-0
DOI: doi: 10.1016/j.surfcoat.2016.08.034
Reference: SCT 21474

To appear in: *Surface & Coatings Technology*

Received date: 11 May 2016
Revised date: 28 July 2016
Accepted date: 15 August 2016

Please cite this article as: C.A. Griffiths, A. Rees, R.M. Kerton, O.V. Fonseca, Temperature effects on DLC coated micro moulds, *Surface & Coatings Technology* (2016), doi: 10.1016/j.surfcoat.2016.08.034

Temperature effects on DLC coated micro moulds

C.A. Griffiths[a], A. Rees[a], R.M. Kerton[a], O. V. Fonseca[b],

[a] *College of Engineering, Swansea University, Swansea SA2 8PP, UK*

[b]*School of Mechanical, Aerospace and Civil Engineering, University of Manchester, Sackville Street, Manchester, M13 9PL, UK*

*c.a.griffiths@swansea.ac.uk

Abstract

Microinjection moulding is a key enabling technology for replicating miniaturized components and parts with functional features at the micrometer and even sub-micrometer length scale. The micro moulding tools used in the process chain are critical for delivering high quality parts for the duration of the product life cycle, and recently tool coatings such as Diamond-like carbon (DLC) have been used to extend their use and enhance the performance. The micro injection moulding process has high injection speeds with cyclic heat transfer characteristics, and little is understood on how the localised heat transfer at the surface will influence the DLC surface coating delamination and cracking. In this research a microinjection moulding process using three different polymers, Polypropylene (PP), Acrylonitrile butadiene styrene (ABS) and Polyether ether ketone (PEEK) is studied. Finite element analysis (FEA) simulation is utilised to identify the process temperature factors that lead to tool thermal expansion and dimensional changes that directly impact the life cycle of the coating. The theoretical and FEA results show that the mould material and the two coatings experience a significantly different thermal expansion from each other. It has also been shown that at the micro scale heat loss at the tool surface is dominant, and the variation in heat has a significant influence on the different thermal expansion rates. In particular the DLC coated micro rib features are particularly susceptible to high variations in heat transfer. The research identifies areas of the tool surface that experience sudden heat variation across the part

surface, and concludes that through process optimisation it is possible to reduce the potential for DLC coating delamination and cracking during service.

Keywords

Micro injection moulding, DLC, FEM, Polymer processing,Thermal stability, Micro fabrication

1. Introduction

The emerging capabilities within the micro manufacturing replication process of micro injection moulding (μ-IM) have enabled the mass production of lighter, thinner and smaller devices for demand led applications within the sectors of healthcare, automotive, communication and consumer electronics [1]. As a result, the technology faces new challenges with regards to the process optimisation, high productivity, advanced mould cavity engineering and precise process control [2, 3]. To meet demand, injection mould machinery manufacturers have developed discrete machines specifically for micro component replication that have added functionality and simplified integration of ancillary processes such as product handling, inspection and packaging [4].

The process of μ-IM has the benefit of replicating a large variety of structured surfaces incorporating functional features within the micro and nano metre range [3]. However, the manufacture of the moulding tools that incorporate micro and nano features and enhance the replication fidelity (RF) at all scales remains a key enabling component of the process chain [3]. Micro moulding tools are manufactured through the innovative combination of complementary micro/nano machining and structuring technologies such as micro electrical discharge machining (μEDM), laser ablation, micro milling and focused ion beam machining [5, 6, 7, 8, 9]. The demand for micro/nano length scale integration features within injection moulding tools results in cavities being produced with technologies that combine so called top-down structuring with bottom-up technologies. The bottom-up technologies allow polymer based self-assembly technologies to deposit on the cavity surface. The deposition of features onto the cavity surface can be used for component surface functionalization or for processing enhancement.

The development of the underpinning micro tooling and subsequent μ-IM polymer replication has been implemented for applications within microfluidic, 'Lab-on-a-Chip' (LoC), inkjet printers, water purification systems, opto-fluidic microscopes, microelectronic cooling, micro chemical reactors and micro fuel cells systems [10]. The μ-IM processes is highly suited for high volume manufacture of these devices which are inexpensive and light weight, and can be considered as disposable alternatives to ceramic platforms. To meet the growing demands within this area requires the key elements of tooling and process to adopt new technologies for higher reliability, higher accuracy and longer life with low maintenance costs. These requirements can be achieved, for example, by modifying the surface of machine elements by adding protective coatings on metal substrates. Thin films are also known as coatings, are layers of material(s) used to protect a part from premature wear resulting from the interaction of the processing environment.

In this paper, the deposition of an amorphous hydrogenated carbon (aC:H) coating on mould surfaces is modelled to determine the effect that cyclic heating and cooling have on the resulting thermal expansion of tooling coating. The paper is organised as follows. The next section reviews surface treatment technologies utilised in tool-making and the functionalities that can be introduced by their application. The subsequent section introduces the theory of thermal expansion. Then, the experimental set-up used to investigate the effects of the μ-IM process on coated mould tools is described. Finally, the experimental results of the simulations are presented and the capabilities of surface treatment of μ-IM tools is analysed.

2. Tooling surface technologies

Traditionally, improving the wear resistance of moulding surfaces was achieved through the application of advanced steels, ranging from ingot cast martensitic matrix steels to advanced powder metallurgy tool steels with a high content of hard carbide particles [11]. However, more recently coating technologies for structured/engineering surfaces have been applied to increase wear resistance and also to functionalise surfaces [12,13-15]. Different manufacturing technologies can be applied to structures and engineering surfaces and they include a broad range of processes. These include sand blasting, innovative grinding systems, focus ion

beam, nano-imprint lithography, chemical texturing and laser machining [13,14,16,17].

2.1 Coated surfaces

Diamond like carbon (DLC) coatings belonged to the amorphous hydrogenated carbon (aC:H) group and are used for the coating of plastic injection moulding inserts [3]. DLC coatings improve the replication performance of the micro and nano structured masters [12]. This is achieved through a combination of superior tribological and mechanical properties such as low friction, low wear and high hardness when compared to traditional tool materials [18,19,20].

The low friction coefficient that results in low wear surface characteristic can be explained with the high ratio between the hardness and Young's modulus and the low ratio between the surface energy and hardness [21]. Typically, the surface treatment of inserts using pulsed laser deposition (PLD) of DLC coatings yields surface hardness of up to 70 GPa with friction coefficients in the range of 0.05–0.2, an order of magnitude lower than that of ceramic coatings [22]. Further investigations of DLC coatings where special attention was paid to the inhibiting role of gas–surface interactions, showed that duty cycles with control variables of time and speed resulted in super low friction coefficients of 0.003–0.008 [23]. In the research conducted by Saha et al. the effect of surface properties of micro structured masters on the hot embossing process was investigated by using nitrogen (N) and nickel (Ni) doped diamond like carbon (N:DLC:Ni) coated and uncoated silicon (Si) micro moulds. The results demonstrated that even with high friction and adhesion characteristics of this replication process the N:DLC:Ni coated Si masters successfully increased the mould lifetime by 3–18 times when compared against uncoated moulds [24].

Bremond et al. studied the tribological behaviour of DLC-coated 100C6 when subjected to a temperature increase from a room temperature to 400 °C. The DLC coatings belonged to the amorphous hydrogenated carbon coatings' group. The results have shown that when used at temperatures higher than 200 °C the coating damage increases significantly due to stiffness reduction of the 100C6-steel substrate [25].

Sasaki et al. investigated the ejection force (F_e) with a consideration of the tool surface roughness and the tool surface coatings [26]. The experimental results demonstrated that when moulding PP and PET a reduced F_e and product deformation were achieved when the surface roughness of the inserts was in the range of Ra 0.212 to 0.026 The PMMA samples required a lower F_e when surface roughness was Ra 0.092. Also, the results showed that any F_e reductions were dependent both on the optimised surface roughness and the polymer material used in the moulding trials. In addition, it was concluded that the PVD WC/C carbon coating was the most effective in reducing Fe [26].

In micro injection moulding, large surface area to volume ratios are typical and result in high adhesion forces between mouldings and the tool surfaces [24]. However, it was reported that by treating the mould surfaces with DLC coatings when moulding PC and ABS polymers a F_e reduction of 40% and 16%, respectively, was achieved in comparison with untreated surfaces [12]. The benefits from using DLC coatings in micro replication processes are proven [24].

2.2 The effects of polymer materials on coating delamination

The ability to predict the interfacial delamination of coatings has a major technical significance with regards to lifetime assessment of products under service conditions. In a study by Di Leo et al. the delamination properties of thermal barrier coatings (TBC) was simulated to determine the relevant material parameters appearing in a traction-separation-type law. The methodology developed in the research is used to determine the material parameters for TBC systems [27]. Kang et al., investigated the delamination of DLC films on titanium alloys. The research concluded that by depositing a TiCN interlayer between the Ti-6Al-4V ELI alloy and the DLC film an improvement in hardness, elastic modulus and interfacial bonding can be achieved. In addition the resulting coefficient to friction was 0.03 ($°C^{-1}$) [28]. Escudeiro et al., studied the wear properties of UHMWPE and PEEK when in contact DLC and Zr-DLC coatings. In the study each material was subjected for 2 million cycles (Mc). The research concluded that Zr-DLC delaminates after 1.2 Mc. The delamination was caused by synergetic stress-induced corrosion which introduces interface fatigue [29].

In a study by Zhang et al., the application of DLC on enhancing the life cycle of artificial joint was investigated when using different substrate materials. In particular, stainless steel, CoCrMo alloy and titanium alloy substrates were used. In the research it was found that the failure mode of DLC coatings on 316 stainless steel and CoCrMo alloy through friction testing was coating delamination. Finally, the report also concluded that DLC coating on Ti6Al4V has superior wear resistance in addition to better stability in immersion and electrochemical tests [30].

3. Thermal expansion

In addition to mechanical interactions such as injection pressure, shear stress, clamping force and friction between the resulting mould surface and polymer melt, the filling (heating) and cooling stages of the process result in cyclical temperature gradients. Delamination of coatings can occur during the transient change of temperature and the thermal expansion variation between the tool and the coating substrate.

3.1 Linear thermal expansion

The change in length that takes place when a solid body is subjected to a change in temperatures depends on the original length of the body and the temperature change over which it is heated or cooled. The relationship between these factors is known as the average coefficient of linear thermal expansion ($\propto_{t_2}^{t_1}$) defined by (Eq. 1) the as:

$$\propto_{t_2}^{t_1} = \frac{L_2 - L_1}{L_R(t_2 - t_1)} \tag{1}$$

where *(t_1)* and *(t_2)* are the initial and final temperatures, *(L_1)* and *(L_2)* are the initial and final lengths, respectively, and *(L_R)* is the length at a reference temperature.

The instantaneous coefficient of linear expansion at any temperature, (*t)*, can be defined by the equation (Eq. 2) as:

$$\propto_t = \lim_{t_1 \to t_2} \left(\frac{L_2 - L_1}{L_R(t_2 - t_1)} \right) = \frac{dL}{L_R(dt)} \tag{2}$$

where *(α_t)* is the instantaneous coefficient of linear expansion at temperature *(t).*

Therefore, the fractional change in length *(ΔL)* of a solid subjected to linear thermal expansion is given by (Eq. 3) as:

$$\frac{\Delta L}{L_0} = \alpha \Delta T \tag{3}$$

where *(α)* is the coefficient of thermal expansion, *(L_0)* is the initial length and *(ΔT)* is the change of temperature to which the material is subjected.

3.2 Superficial thermal expansion

As section 3.1 has proven due the thermal expansion of the tooling during processing the resulting tooling dimensions will be subjected to superficial thermal expansion. Through utilising the terms of (Eq. 3) the calculation can be expanded to incorporate the new superficial change in length (*L*). By defining a new representation of new superficial length *(L)* using the terms of equation (Eq. 3). Since $L = L_0 + \Delta L$, the final length *(L)* can be defined by a new equation (Eq. 4) as:

$$L = L_0 + L_0 \alpha \Delta T = L_0(1 + \alpha \Delta T) \tag{4}$$

A rectangular micro rib feature with an area *(A_0)* that can be obtained by the product of its height *(H_0)* and its width *(W_0)*. The effect of the temperature in both *(H_0)* and *(W_0)* result in new area defined by the following equation:

$$A = HW = H_0(1 + \alpha \Delta T) W_0(1 + \alpha \Delta T) = H_0 W_0 (1 + \alpha \Delta T)(1 + \alpha \Delta T)$$
$$A = A_0[1 + 2\alpha \Delta T + (\alpha \Delta T)^2] \tag{5}$$

Since the value of *(α)* is typically small and for small temperature change *($\alpha \Delta T$)* is significantly less than 1. Therefore, the term *($\alpha \Delta T)^2$* in the previous equation is negligible compared to the *($2\alpha \Delta T$)* term. Hence, the following equation defines the new area of an object subjected to thermal expansion, which is given by:

$$A = A_0(1 + 2\alpha \Delta T) \tag{6}$$

As film-substrate structures can be used over a wide variety of applications it is important to investigate their behaviour not just within a mechanical regime but also the effect of the coating when subjected to transient change in temperature and varying thermal expansion between the tooling material and the coating. During the process of µ-IM high variations in temperature hysteresis profiles are witnessed through cyclic heating and cooling stages and localised shear heating. In addition, the processing temperature of the polymer melt also modifies the thermal footprint of the process. Also due to the inherent volumetric change during the processing of polymers through µ-IM interactions occur between processing variables such as injection pressure, shear stress, clamping force and friction between the resulting mould surface and polymer melt. Therefore, this study presents a novel approach at investigating the effect that the thermal and processing variables have on the resulting delamination of a DLC coating. In particular, the investigation analyses the difference in thermal expansion between the polymer melt, Starvax ESR stainless steel substrate and coating film has on the delamination process.

4. Experimental set-up

4.1 Part design

The part design used in this study is a 15 × 20 × 1 mm micro-fluidics platform (Fig.1). The system design includes features commonly found in micro-fluidics components such as reservoirs, channels and waste compartments. The pin dimensions are 500µm in diameter and 600µm in height, and the cross section of the main channels is 200 ×100 µm. The mould material used is Starvax ESR stainless steel, Table 1 shows the material properties.

Table 1. Physical properties of Starvax ESR stainless steel

Temperature *(°C)*	20	200	400
Density *(kg/mm^3)*	7,800	7,750	7,700
Modulus of elasticity *(N/mm^2)*	200, 000	190, 000	180,000
Coefficient of thermal expansion *($°C^{-1}$)*	-	$11.0x10^{-6}$	$11.4x10^{-6}$

Figure 1

Figure 1. Illustration (a) microfluidic part and (b) micro-mould.

4.2 DLC Coating specification

A double layer coating technique was used to improve the coating adhesion between the thin films deposition and the substrate (Fig 2). Initially, the substrate was coated with an intermediate layer of silicon carbide (Si-C:H) to a thickness of 0.5µm. Following this a 2µm DLC thin film was deposited onto the first layer at a low frequency of 320 W, at 645 V, under a working pressure of 4Pa and with 20% of H_2 in (C_6H_{12} + H_2) gas mixture using a PACVD machine.

Testing of the coatings were performed with the values displayed in Table 2. Hardness and Young's modulus were obtained by a nano-indenter CSEM nano-hardness tester using a Berkovitch diamond tip. The Oliver and Pharr method was used to calculate the values and correspond to an average of 30 indentations with penetration depths <10% of the thickness of the sample. Friction measurements were preformed using a ball-on-disc tribometre. An 8-mm Al2O3 ball was used as the mating material and a 5-N load was applied on the system (Hertz pressure=950 MPa). The sliding speed was kept at 0.17 m/s for a fixed number of 100,000 cycles. Tests were performed in normal atmosphere and no lubricant was used.

Figure 2

Figure 2. Coating deposition configuration

Table 2. Mechanical properties of DLC coating.

Properties	Typical Value
Micro-hardness (GPa)	22 ± 2
Coefficient of Friction ($°C^{-1}$)	0.05
Young Modulus (GPa)	160 ± 10
Wear Rate ($mm^3\ N^{-1}\ m^{-1}$)	$5x10^{-7}$

4.3 μ-IM simulation

For this research finite element analysis (FEA) using Autodesk Simulation Moldflow Insight/Synergy 2014, was used to study the temperature effects on the mould surface due to melt flow behaviour of three polymers materials: PP, ABS and PEEK. This FEA software is a graphical user interface which permits the simulation and subsequent post-processing analysis of polymer processing data. Initially, a CAD model was imported and meshed to provide accurate simulation conditions (Fig.3). Each polymer was then simulated under the high speed manufacturing processing conditions displayed in Table 3. During the simulations the highest and lowest recommended Melt temp (T_b) were used, the Mould temperature (T_m) is based on the recommended temperature for each polymer were used. Originally a fixed V_i based on a filling of 0.25s giving an injection, packing and cooling time of 8 seconds and an overall cycle time of 13 seconds. The research will later show that the V_i had to be modified in order to optimise the filling effects on temperature.

4.4 Bulk temperature at end of fill

To analyse the melt flow behaviour a dual domain based on Hele Shaw was utilised within the FEA software. To investigate the melt flow behaviour the influence of the polymer bulk temperature was chosen as opposed to the simple average temperature. As the temperature of the polymer melt changes as a function of time, location and part thickness, the bulk temperature simulation is used to indicate the weighted average temperature across the part thickness. In addition, by applying the bulk temperature simulation it is possible to identify the energy being transported through a particular location within the part.

4.5 Part and Cavity surface Temperature Results

This result is interested in identifying the temperature at the mould surface, it shows the temperature of the plastic and DLC interface. Generally this would be used for identifying areas of temperature and cooling imbalance for the prevention of part warpage. In this research the Part and Cavity surface Temperature Results will be compared to bulk temperature results. The polymer and DLC temperatures can be different from the bulk temperature due to the heat transfer coefficient. This

difference will be critical for determining the thermal expansion at the surface of the mould and will also look at the influence of the extremes of the process and the frozen layer of the polymer at the tool surface.

4.6 Frozen layer fraction at end of fill

The frozen layer result represents the thickness fraction of frozen layer at the end of filling. Polymers are considered frozen when their temperature falls below the transition temperature (T_{trans}). The heat transfer from the part to the mould surface is very short as the mould cools the surface of the part. Once filling stops the heat loss through the part thickness is completely dominant in that area, and cooling of the part at the surface acts as an insulator reducing any further heat transfer from the polymer to the mould. This research will simulate the frozen layer fraction at end of filling stage.

Figure 3

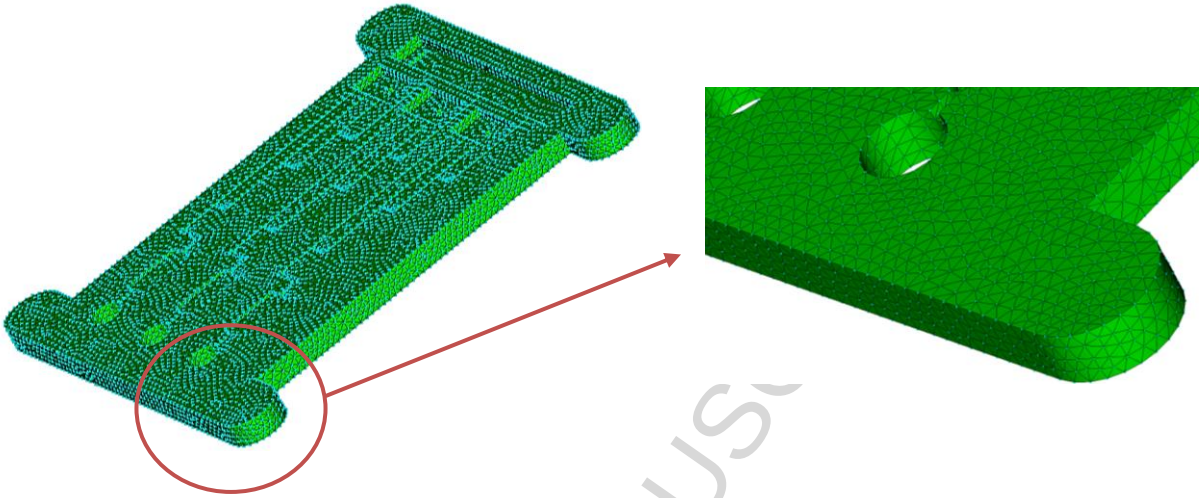

Figure 3. FEA Mesh of the microfluidic part.

Table 3. Simulation processing data

Characteristics	PP	ABS	PEEK
Material Properties			
Type	Crystalline	Amorphous	Crystalline
Trade name	Polypropylene PPC 4660	Magnum 8434	Victrex PEEK 150CA30
Manufacturer	Total Petrochemicals	Styron EUR	Victrex USA
Mould Temperature (°C)	30	50	190
Melt Temperature Range (°C)	190 - 270	240 – 270 (Optimised to 260)	375 - 400
Transition Temperature (°C)	120	90	308
Ejection temperature (°C)	80	85	296
Viscosity (Pa s)	0.32	0.28	0.51

5.0 Results & Discussion

5.1 Linear thermal expansion during processing

Inputting the upper limit of the temperature ranges detailed in Table 3. The fractional change in length *(ΔL)* can be calculated using equation (Eq. 3) for the micro mould configuration in Figure 2. The results are displayed graphically in Figure 4.

Figure 4

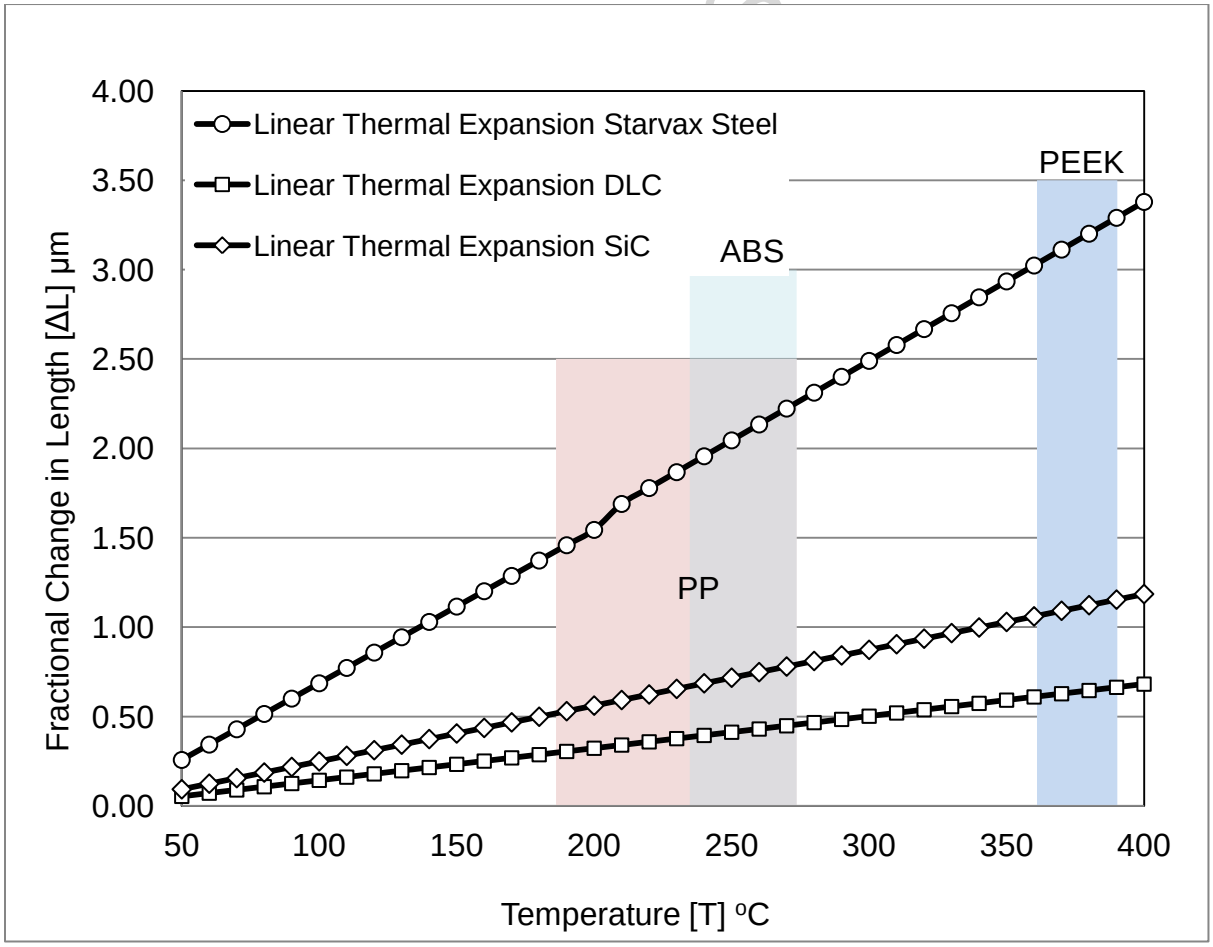

Figure 4. Linear Thermal Expansion for DLC coating, Si-C:H intermediate layer and Starvax ESR steel substrate.

From the results displayed in Figure 4 one can conclude that Stavax ESR substrate, the Si-C:H intermediate layer and the DLC coating witness differing dimensional changes during thermal cycles. Moreover, Figure 4 shows that there are not only

different fractional changes in length for the materials but also they are growing at different rates. These results are undoubtedly caused by the effect of different thermal expansion coefficients of the corresponding tooling coating components. Therefore, this phenomenon can cause microstructural problems that could lead to the mismatch between the tool substrate and the coatings. This could result in the formation of residual stresses in the coating that may cause micro-cracking, adhesion loss, detachment or delamination of the coating. Figure 4 also displays the suggested T_b ranges for three different polymer materials, PP, ABS and PEEK. The result in Table 4 shows that if one chooses to inject PEEK into the micro-mould the expansion is between 3.11 - 3.37 µm and within the same temperature and it can be seen that DLC will have a ΔL of 0.62 – 0.68 µm. The difference between the changes in length for the substrate compared to the DLC coating is around 2.5 µm in this case. It is also shown in Table 4 that even within a given process window there is a difference in the change in length. PP has the widest process window, and within this range the steel and DLC will experience a change in ΔL of 0.76 µm and 0.14 µm respectively. The thermal expansion variations for the three materials could lead to failure in service and further validation is necessary.

Table 4. Tool and surface treatment change in ΔL from ambient

Material	PP (190-270°C)	ABS (240-270°C)	PEEK (375 - 400°C)
	Change in ΔL [µm] from ambient temperature		
Steel	1.4 - 2.2	1.95 - 2.22	3.11- 3.37
Si-C:H	0.53 - 0.78	0.68 - 0.78	1.09 - 1.18
DLC	0.30 - 0.44	0.39 - 0.44	0.62 – 0.68
	Change in ΔL [µm] with in the recommended T_b ranges		
Steel	0.76	0.27	0.26
Si-C:H	0.25	0.1	0.09
DLC	0.14	0.05	0.05

5.2 Superficial thermal expansion during processing

For superficial thermal expansion practical purposes, the coating of the micro-object will be assumed to be a single 2.5 µm layer of DLC coating and the Figures shown in Table 5.

Table 5. Thermal expansion results

Thermal expansion	
Linear	Superficial
Room temperature T_0 = 20°C.	
α_{Subs} = 11 x 10^{-6}°C^{-1} for Temperatures from 20°C to 200°C and α_{Subs} = 11.4 x 10^{-6}°C^{-1} for Temperatures greater than 200°C	
α_{DLC} = 2.3 x 10^{-6}°C^{-1}	
L_0 = 780μm for both DLC coating and substrate, see Figure 5 (b).	DLC coating thickness = 2.5μm.
$\alpha_{Si\text{-}C:H}$ = 2.3x10^{-6}°C^{-1}	W_0 = 780μm and H_0 = 97μm for DLC coating, see Figure 5 (b).
	W_0 = 775μm and H_0 = 92μm for the Substrate.

Figure 5 shows two illustrations of a micro-tool and the selection of a rectangular micro-object inside it, which will be subjected to the thermal expansion analysis in this study.

Figure 5

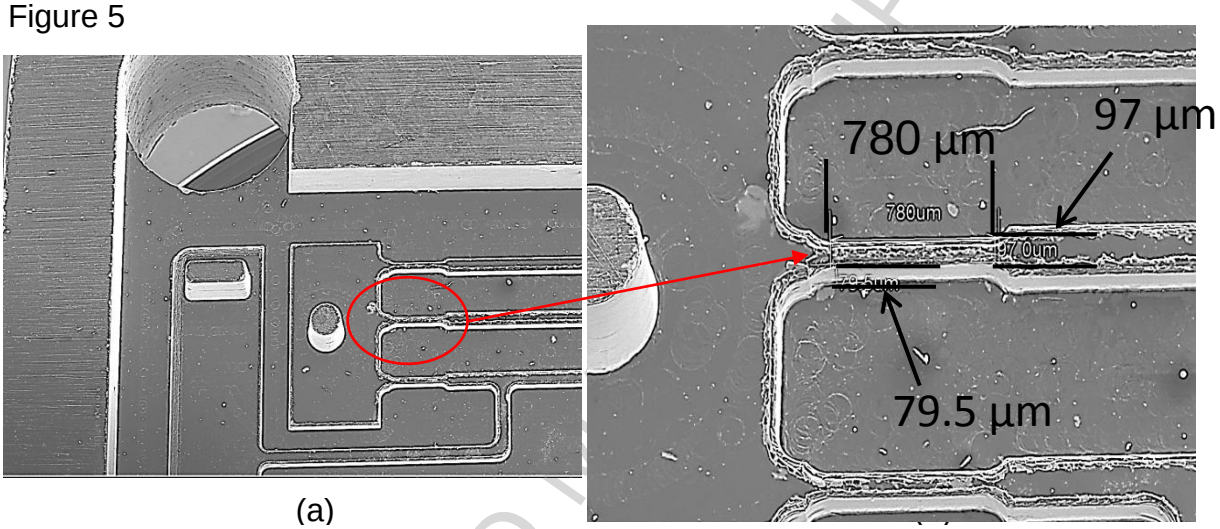

(a)

Figure 5. (a) SEM image of the micro-mould at 20kV and 15x magnification and (b) micro-channel dimensions at 20kV and at 45x magnification.

The result in Figure 6 shows the effects of temperature on the different components of the micro-mould. It is shown that the tool and coating will follow different superficial growth gradients. The Figure 6 shows a slope of 1.64 μm^2 for the mould material which is greater than a slope of 0.35 μm^2 for the DLC coating. The phenomenon of dissimilar expansion due to temperature cycles could lead to bending and/or compression effects on the coating layer caused by growth of the substrate that may result in chipping, bonding and damage of the coating. On the other hand, it might also be expected that changes in temperature do not importantly affect the coating surface of a tool. This can be possible due to excellent adhesion strength of the DLC to the substrate. Also, hard coatings, such as DLC thin films may absorb deformations caused by temperature changes due to elastic properties.

Figure 6

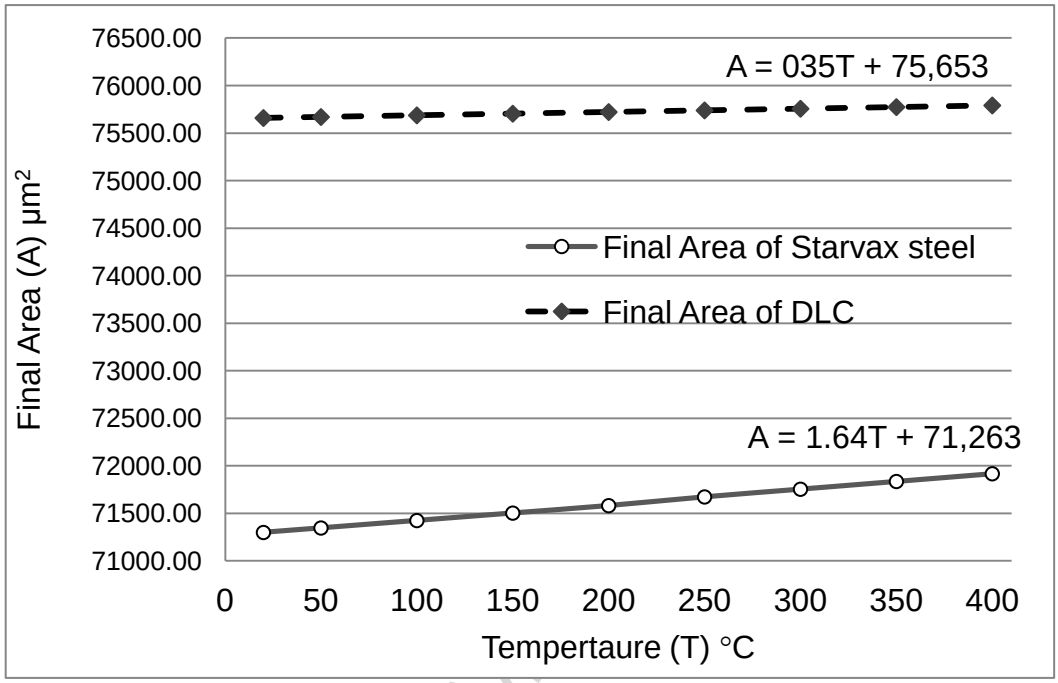

Figure 6. Superficial thermal expansion of DLC coating and Starvax ESR steel substrate.

5.3 Finite element analysis

In addition to investigating the resulting thermal expansion of tooling coatings this study expands the analysis to consider the influence of the polymer melt temperature. In particular, Autodesk Simulation Moldflow Insight/Synergy 2014 was employed to run a finite element analysis of the resulting flow behaviour of PP. ABS and PEEK melts.

5.3.1 Bulk temperature FEA analysis

Process setting influence on bulk temperature

Bulk temperature is defined as the average temperature across the thickness of a part and is a very important parameter during injection moulding processes. It shows the energy that is transported through a particular location and accurately reflects the average temperature of a moving fluid. It is a relevant study area for this research as it identifies temperature changes with time and location, but also with thickness thus making it of major relevance particularly when using coated tooling. The simulation results show that the maximum bulk temperature for PP was 271.3 °C, for ABS at 262.3 °C and for PEEK at 406.4°C. These values were in all cases, higher than the melting temperatures specified at the beginning of the simulations, i.e. 270 °C for PP, 260 °C for ABS and 400 °C for PEEK. This is due to the high V_i (0.25 s) at the filling stage increasing the shear rate causing a reduction in the viscosity. The simulation considers the maximum and minimum temperatures for high T_b and low T_b settings for each of the materials. The results in Figure 7 show that there is a wide temperature distribution. In particular the highest difference is 82 °C (70 % difference) for PP, 61.5 °C (76 % difference) for ABS and 138.6 °C (66 % difference) for PEEK. The results confirm a temperature difference within the part, however it is unclear from this result how much of this variation is experienced at the mould surface.

Figure 7

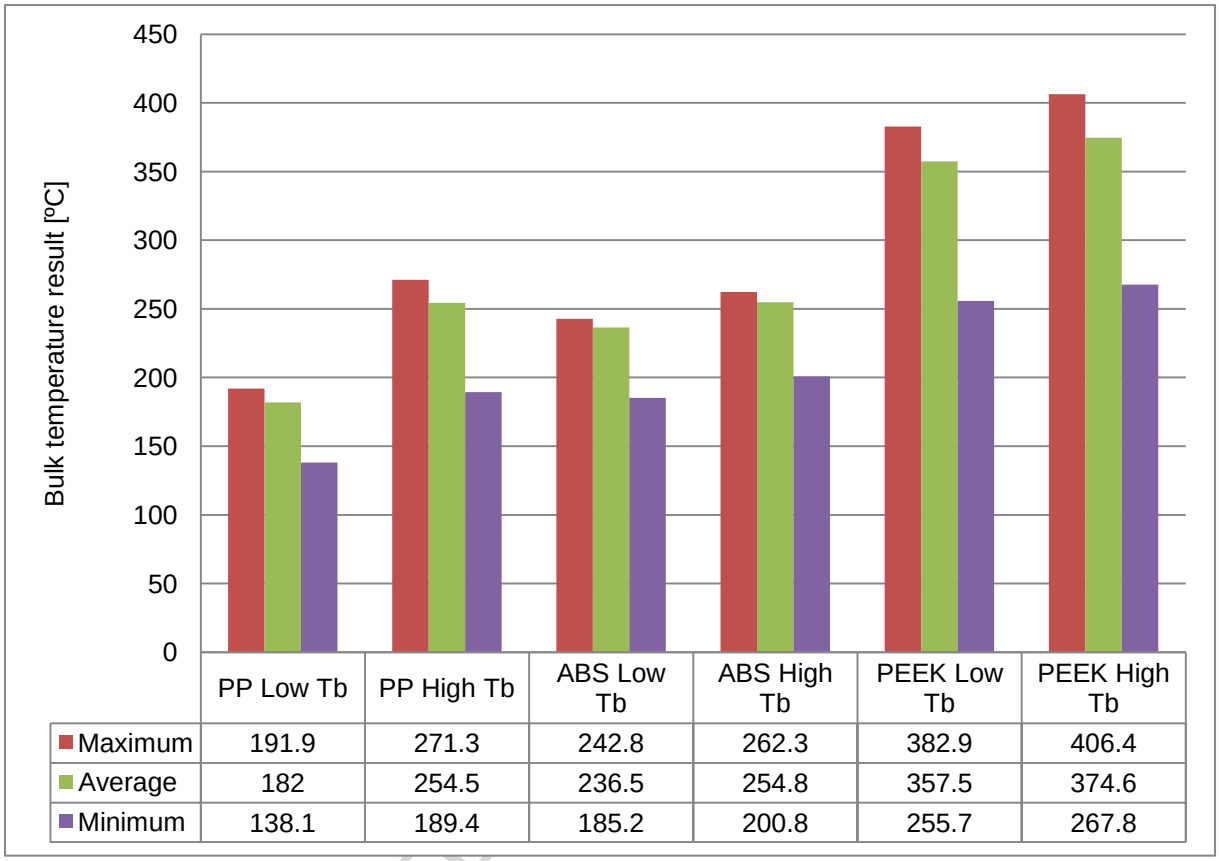

	PP Low Tb	PP High Tb	ABS Low Tb	ABS High Tb	PEEK Low Tb	PEEK High Tb
Maximum	191.9	271.3	242.8	262.3	382.9	406.4
Average	182	254.5	236.5	254.8	357.5	374.6
Minimum	138.1	189.4	185.2	200.8	255.7	267.8

Figure 7. Bulk temperature results for PP, ABS and PEEK

Bulk temperature distribution across the part result

To establish the variation in the bulk temperature, the distribution at the end of filling across the part is shown in Figure 8. In the ABS example shown, the red colour indicates the highest bulk temperature at the end and green and yellow indicate the lowest temperature. Ideally a uniform bulk temperature distribution during filling is desirable for mould and part design. It is clearly seen in Figure 8 that there is a different distribution of temperature on the part. The main temperature variations can be located at the polymer entry point and central flow region of polymer (Fig 8b). These hot spots are due to excessive viscous heating during the filling stage. The ABS results are typical and they demonstrate the different temperature ranges across the part (85 - 243 ºC for the low T_b and 91 - 262 ºC for the high T_b). The distributions identify regions of localised change in the bulk temperature resulting in the potential for localised areas of thermal expansion of the mould material. As

shown in the thermal expansion distributions across the microfluidic channels (X1-X1 in Figure 9 and the gate entry point (X2-X2) in Figure 10, these localised areas are identified as critical for the study of DLC damage and delamination.

Figure 8

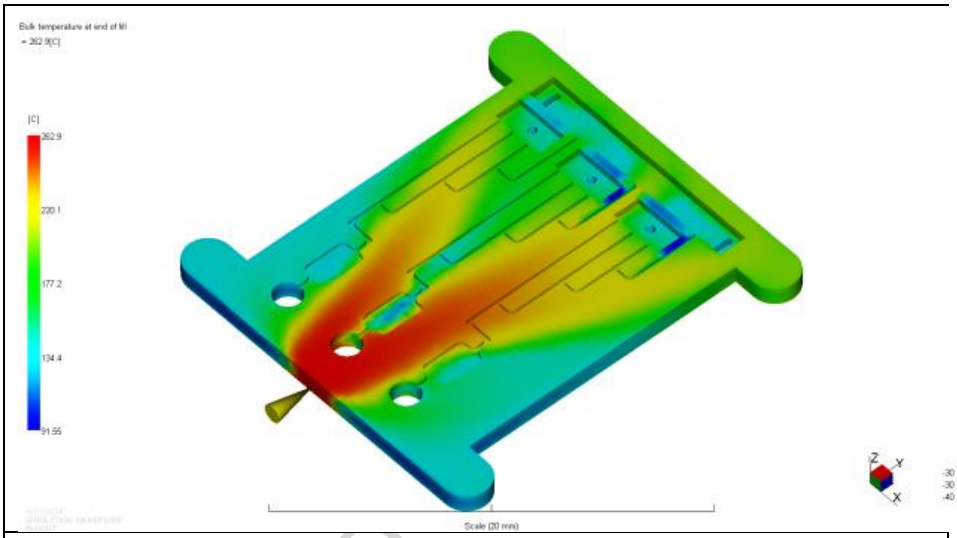

(a) ABS High setting with a 91 - 262 ºC distribution

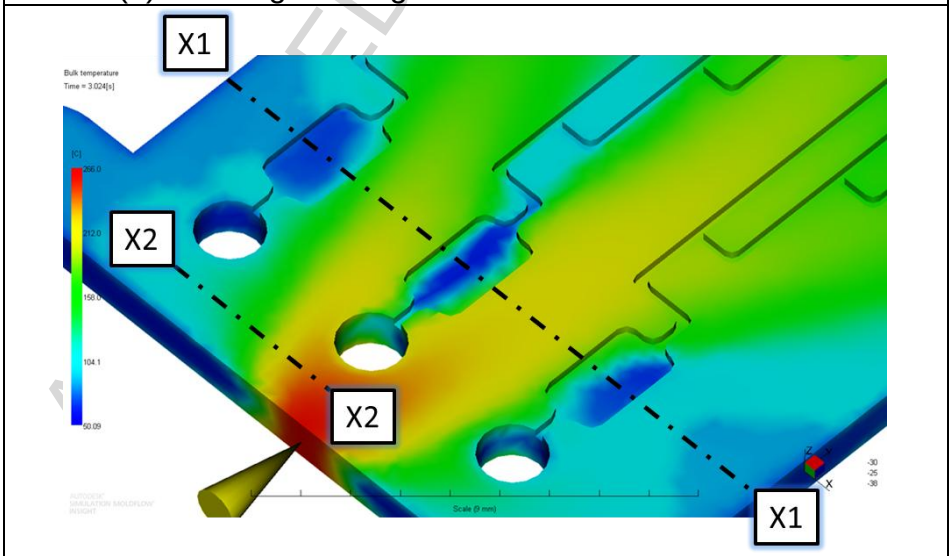

(b) Distribution across the entry point and microfluidic channels

Figure 8. Bulk temperature distribution at the end of the fill for ABS.

Figure 9

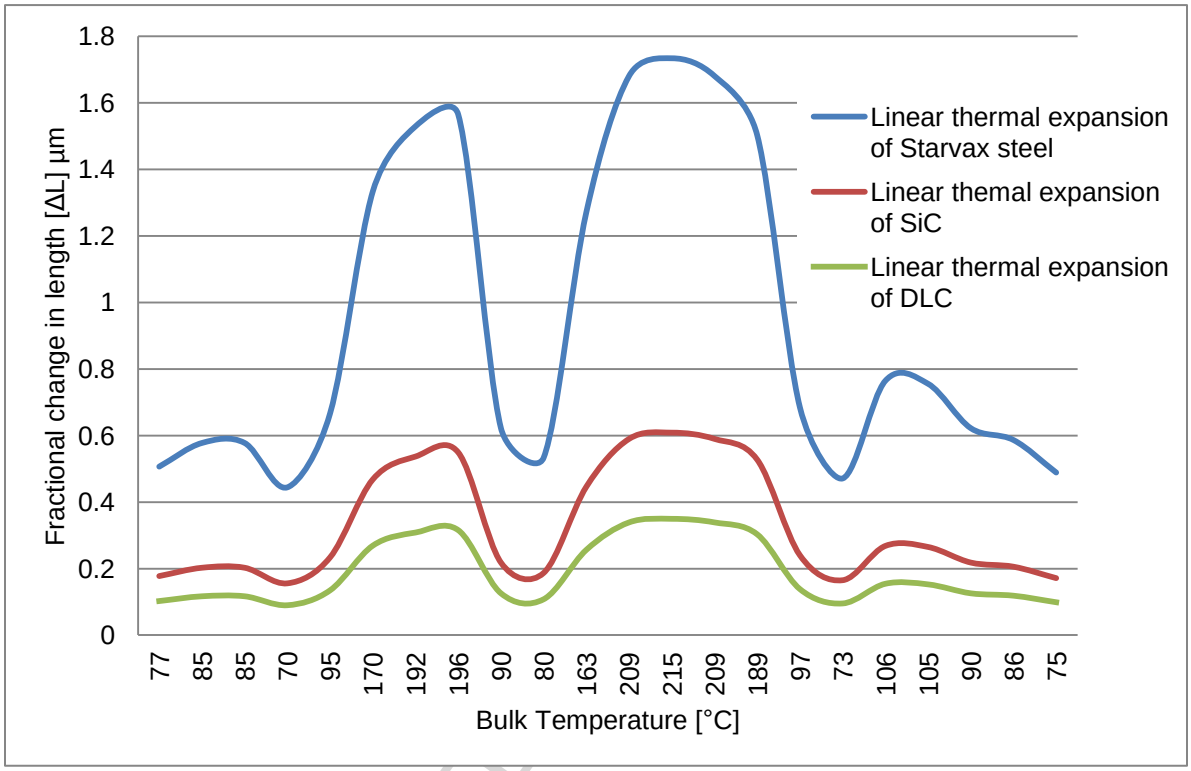

Figure 9. Thermal expansion distribution across the microfluidic channels(X1-X1)

Figure 10

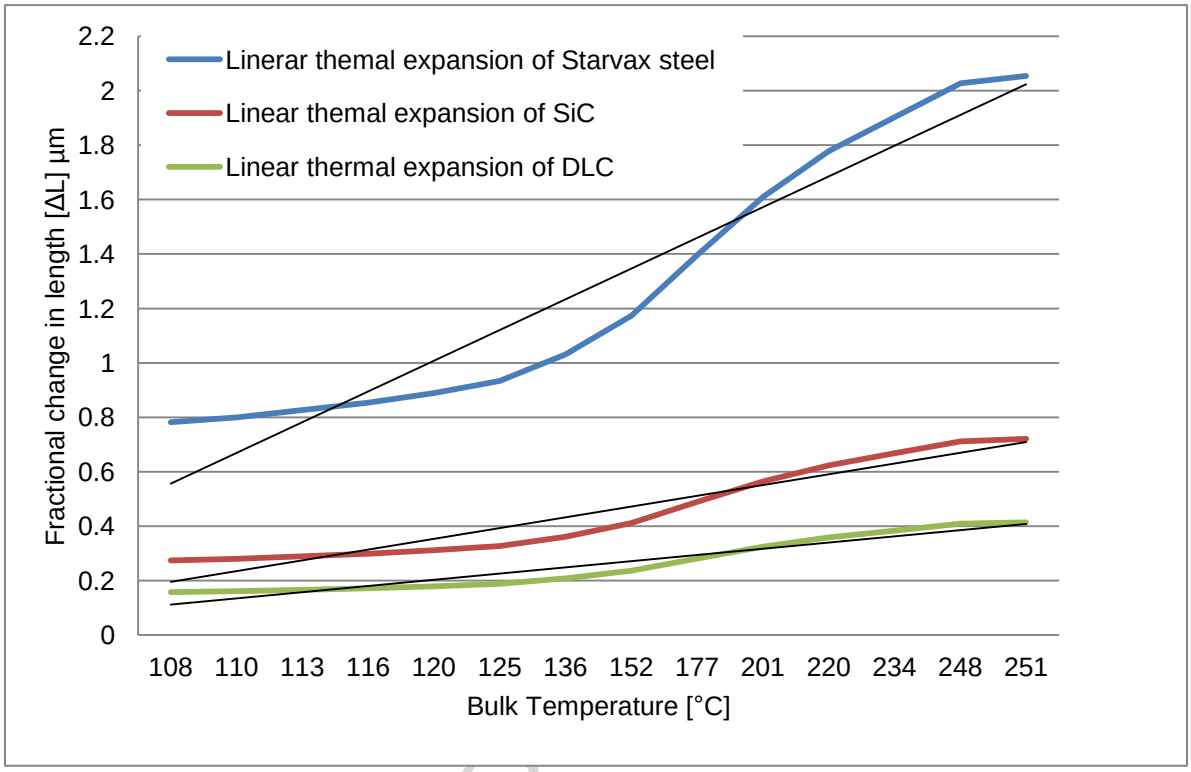

Figure 10. Thermal expansion distribution across the gate entry point (X2-X2)

5.3.2 Part and Cavity surface Temperature Results

It has been shown that there is a wide variation of bulk temperature experienced by the part during processing. This variation is due to the process settings used (Table 3) and also due to the geometry of the part. The research is interested in the influence on temperature fluctuation experienced by the DLC surface treatment. Therefore, to differentiate between the bulk temperature of the part and the temperature experienced at the mould, further surface temperature results are analysed.

The simulation considers low and high T_b settings and Table 6 confirms a temperature variation between the settings (PP has the highest part and cavity surface temperature variation with a difference of 27.1% and 25.3% respectively). Importantly the simulation identifies that the surface temperature differences between the part and cavity are very small (<5%). But it also shows that these temperatures are below the original T_b setting by between 59-67% for all three

materials. This result would suggest that the surface temperatures are much lower than those shown in the bulk temperature results (Fig 7) and that the thermal expansion ranges that the DLC experiences will not be as extreme.

The assumption with the surface simulation results is that at the macro scale there is a large layer of frozen polymer at the mould part interface that is preventing bulk heat transfer of the part to the mould surface. This assumption can be based on moulds being cooled via water channels and slow injection speeds allowing for the frozen layer to develop. Neither of which cannot be said for µ-IM. Micro parts have a higher surface to volume ratio than meso parts and rapid heat loss is experienced through heat transfer into the mould surface. Figure 11 shows a post filling heat distribution, the results for both the part and mould show a central area of increased heat, this is to be expected. The result also correctly shows that the high surface to volume ratio area on the micro channels are cooled on the parts and that the micro channel that produce the ribs on the tool have an increased temperature.

We must assume that the frozen layer at the surface is not developed sufficiently to act as an insulator and that the bulk temperature variations (Figure 7 and 8) are accurately experienced at the DLC surface. To confirm this, the frozen layer is studied and a further simulation with settings that would promote a layer are performed.

Table 6. Summary of cavity temperature results at high V_i and a 13 second cycle time

Temperature results [°C]	PP [T_b]		Diff] %	ABS [T_b]		Diff %	PEEK [T_b]		Diff %
	190	270		240	270		375	400	
Part surface max	67.2 (<64% T_b)	87.7 (<67% T_b)	27.1	87.7 (<63% T_b)	90.2 (<66% T_b)	8.2	153.2 (<59% T_b)	162.4 (<59% T_b)	13.0
Part surface min	63.9	82.8		82.8	86.0		141.2	149.5	
Cavity surface max	64.1	83.0	25.3	83.0	86.1	7.2	141.8	150.2	9.6
Cavity surface min	62.0	79.9		79.9	82.9		135.7	143.6	
Average mould exterior	60.8	78.3	22.3	78.3	81.2	3.5	132.2	139.9	5.5
Heat removal through the outer boundaries [kW]	0.0054	0.0080	32.5	0.0080	0.0084	4.7	0.0161	0.0172	6.3

Figure 11

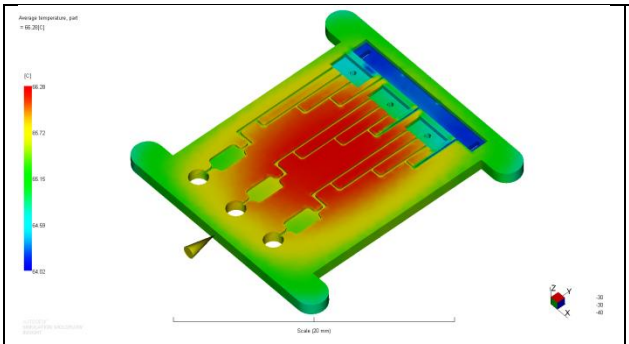

(a) PP Part temp distribution

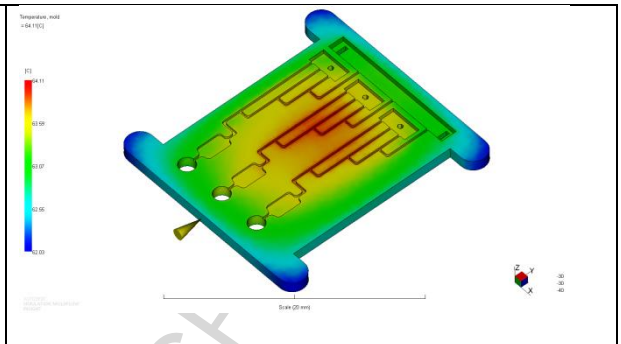

(b) Mould temperature distribution

Figure 11. Part and Mould surface temperature distribution after filling.

5.3.3 Frozen layer fraction at end of fill result

During the filling stage of the moulding process the temperature of the polymer in contact with the mould decreases. When the polymer melt temperature falls below T_{trans} a frozen layer forms where a higher value indicates a thicker frozen layer. In this research the frozen layer analysis is a measure of heat transferred by the conduction of the polymer melt (T_b). The degree of frozen layer formation will directly influence the temperature transfer between the polymer melt and moulding surface. The insulation properties due to frozen layer formation will influence the rate of expansion and contraction of the mould surface coatings. Importantly the rate at which heat moves from the part to the DLC surface is affected by the material thermal conductivity properties. PEEK has a higher thermal conductivity (0.542 (W/(m·K)) @ 308˚C) than PP (0.1762 (W/(m·K)) @ 230˚C) and ABS (0.152 (W/(m·K)) @ 240˚C), meaning that the frozen layer thickness of PEEK act as less of an insulator than PP and ABS.

The simulated surface temperature results in identified temperatures below the bulk temperature. To demonstrate the presence of a frozen layer in µ-IM further simulations are performed with V_i as a control factor. The results shown in Table 7 are important in identifying that at the high V_i associated in µ-IM there is a low to no presence of a frozen layer. By increasing the injection time to 2 seconds a frozen layer is seen to increase for all materials. To highlight the importance of optimizing the process window using V_i to control the frozen layer, the simulation results showed that it was not possible to fill the PEEK part using a 2 second injection time. Only by reducing the time was it possible to fill the part.

Ideally the frozen layer should be constant thickness for ideal filling. A varying frozen thickness variation across the part is observed. The heat transfer relationship with the frozen layer influence is confirmed with a time to reach ejection temperature result. Figure 12 shows that the high surface to volume ratio micro features have reached a cooling temperature (T_{trans}) before the main body of the part. This result confirms heat transfer to the mould surface and it further identifies interface regions of material expansion and contraction.

Table 7. Frozen layer fraction using V_i control

Frozen layer fraction	PP		ABS		PEEK	
	0.25 Vi	2 V_i	0.25 V_i	2 V_i	0.25 V_i	2 V_i
maximum	0.26	1.0	**0.0**	1.0	1.0	1.0
minimum	**0.0**	**0.0**	**0.0**	**0.0**	**0.0**	0.036
average	0.09	0.62	**0.0**	0.0071	0.31	0.79

Figure 12

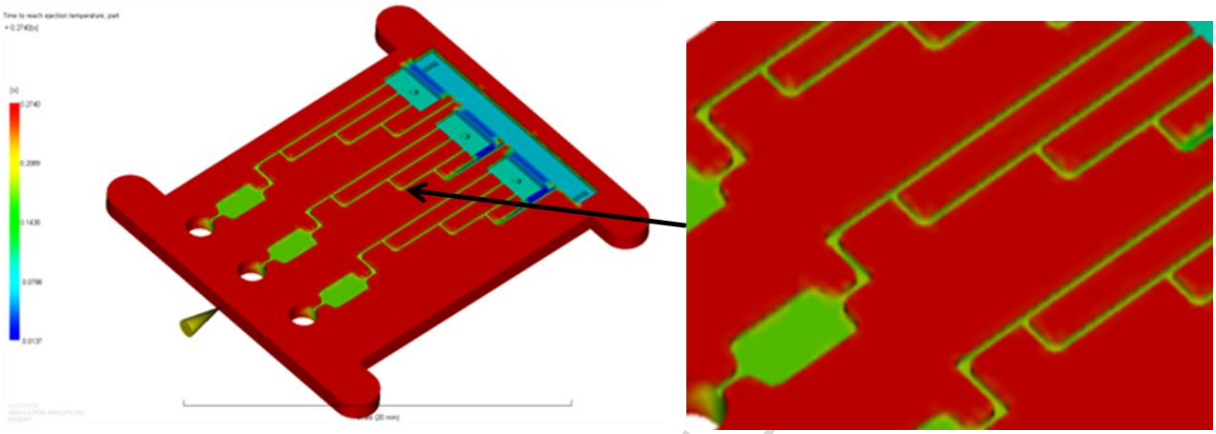

Figure 12. Ejection temperature result for main body and micro scale features

6. Conclusions

The potential of DLC coatings for improving the manufacturability of parts using µ-IM process has previously been demonstrated. The investment into surface treatment technologies particularly relatively new ones requires a consideration of the life span of the treatment and failures in service. The investigated surface treatment considers a steel mould with two CVD based depositions. Each of the three materials has a different thermal expansion, and this difference is a potential failure mechanism leading to cracking of the coating and delamination from the mould. The research looks at the simulation of high speed µ-IM process used to produce a micro part in three different polymer materials. The simulation model is used to identify the process temperature factors that lead to tool thermal expansion and dimensional changes that impact the life of the coating.

- The three polymers have different processing range of T_B and T_m values, and the research looked at the theoretical influence of these values on the linear and superficial thermal expansion. The results show that the mould material and the two coatings experience a significantly different thermal expansion from each other. Within the processing range of each polymer material an expansion of up to 3.4 µm can be expected for the steel and up to 1 µm for the surface treatments. The differences can result in the generation of very high stresses in the coating that may lead to delamination, cracking and coating failure. It should also be noted that the same mould can be used for a variety of materials, and in the case of the three selected there is clearly a wide variation. Adhesion of thin films on a substrate requires that the tooling material needs to be more thermally aligned with the thermal properties of coatings. This is not always possible so optimisation of the moulding process can be used to reduce the expansion.

- FEA analysis of the µ-IM process is critical for design optimisation. The bulk temperature at the end of the filling stage result is used to calculate the theoretical heat transfer related expansion. In particular the bulk temperature is used to identify the minimum and maximum temperature experienced by

the parts and is also used to identify regions within the part where thermally induced expansion is critical. It is shown that the filling region of the part is particularly sensitive to bulk temperature changes.

- The mould material is coated by 0.5 μm thick of silicon carbide to enhance the adherence of a second layer of DLC coating of 2μm thickness. To establish if the observed high bulk temperature is actually experienced at the surface of the mould the FEA model is used to investigate the frozen layer fraction at the mould and melt interface. The frozen layer thickness is a fraction of the part thickness. A higher value represents a thicker frozen layer and a polymer is considered to be frozen when the temperature falls below the transition temperature (T_{trans}). At the meso scale one can expect a fully formed frozen layer and this layer will result in a reduction of bulk temperature transfer to the DLC surface. However, the process being modelled is high speed μ-IM where a higher part surface to volume ratio and the extremely high injection speeds (0.25 s) will prevent the formation of the frozen layer. The part and mould surface results showed a reduction in temperature, but to evaluate if the bulk temperature variations are experienced at the DLC surface further simulations that modified the frozen layer using V_i control are performed. The results show that at high speed filling a layer is not fully formed thus proving that the DLC does experience a high expansion. The frozen layer results are also compared the high time to reach ejection temperature results. The observed high time to reach T_{trans} confirms that heat transfer is experienced through the tool surface.

- To emphasise the sensitivity of heat loss through the tool surface and viscosity at the micro scale, it could be seen that by increasing the frozen layer by reducing V_i it was no longer possible to fill the PEEK parts and a short shot result was observed. Viscosity exponentially increases with decreasing temperature and thus fluidity and the inability to fill. This result confirms that the high settings required to fill the micro part result in a temperature transfer at the melt interface.

- It has been shown that at the micro scale heat loss at the tool surface is dominant and the variation in heat has a significant influence on the different thermal expansion rates. In particular the size effect of DLC coated micro rib features are particularly susceptible to high variations in heat transfer and are thus areas of interest for observing coating delamination and cracking.

- Micro part and mould design should consider process and part optimisation in terms of reducing the amount of heat experienced at the tool surface and reducing sudden heat variation across the part surface. This must be balanced with optimisation of the filling and the part frozen layer. A special consideration of maintaining a constant part thickness for balancing the heat loss, and reducing thermal expansion at the mould surface.

Acknowledgements

The authors would like to acknowledge the support of the Advanced Sustainable Manufacturing Technologies (ASTUTE) project, which is part funded from the EU's European Regional Development Fund through the Welsh European Funding Office, in enabling the research upon which this paper is based. Further information on ASTUTE can be found at www.astutewales.com.

References

[1] Ch. Hopmann, T. Fischer, New plasticising process for increased precision and reduced resistence times in injection moulding of micro parts, CIRP Journal of Manufacturing Science and Technology, Volume 9, May 2015, Pages 51-56, doi:10.1016/j.cirpj.2015.01.004

[2] Shia-Chung Chen, Yi Chang, Yeon-Pun Chang, Yen-Chen Chen, Chia-Yen Tseng, Effect of cavity surface coating on mold temperature variation and the quality of injection molded parts, International Communications in Heat and Mass Transfer, Volume 36, Issue 10, December 2009, Pages 1030-1035, ISSN 0735-1933, http://dx.doi.org/10.1016/j.icheatmasstransfer.2009.06.020.

[3] C.A. Griffiths, S.S. Dimov, A. Rees, O. Dellea, J. Gavillet, F. Lacan, H. Hirshy, A novel texturing of micro injection moulding tools by applying an amorphous hydrogenated carbon coating, Surface and Coatings Technology, Volume 235, 25 November 2013, Pages 1-9, ISSN 0257-8972, http://dx.doi.org/10.1016/j.surfcoat.2013.07.006.

[4] C. A. Griffiths , G. Tosello, S. S. Dimov, S. G. Scholz, A. Rees, B. Whiteside, Characterisation of demoulding parameters in micro-injection moulding, Microsystem Technology, July 2014, ISSN 0946-7076, http://dx.doi.org/10.1007/s00542-014-2269-6

[5] Williams, E., Brousseau, E.B., Rees, A., Nanosecond Yb fibre laser milling of aluminium: effect of process parameters on the achievable surface finish and machining efficiency, The International Journal of Advanced Manufacturing Technology, Volume 74, Issue 5-8, pp 769-780, September 2014, http://dx.doi.org/10.1007/s00170-014-6038-6

[6] Rees, A., Brousseau, E., Dimov, S.S., Bigot, S., Griffiths, C.A. Development of surface roughness optimisation and prediction for the process of wire electro-discharge grinding, The International Journal of Advanced Manufacturing Technology, Volume 64, Issue 9-12, pp 1395-1410, February 2013, http://dx.doi.org/10.1007/s00170-012-4110-7

[7] S.G. Scholz, C.A. Griffiths, S.S. Dimov, E.B. Brousseau, G. Lalev, P. Petkov, Manufacturing routes for replicating micro and nano surface structures with bio-mimetic applications, CIRP Journal of Manufacturing Science and Technology, Volume 4, Issue 4, 2011, Pages 347-356, ISSN 1755-5817, http://dx.doi.org/10.1016/j.cirpj.2011.05.004.

[8] V. Velkova, G. Lalev, H. Hirshy, F. Omar, S. Scholz, E. Minev, S. Dimov, Process chain for serial manufacture of 3D micro- and nano-scale structures, CIRP Journal of Manufacturing Science and Technology, Volume 4, Issue 4, 2011, Pages 340-346, ISSN 1755-5817, http://dx.doi.org/10.1016/j.cirpj.2011.03.005.

[9] Rees. A, Dimov. S.S, Ivanov. A, Herrero. A, Uriarte. L.G, (2007), “Micro-EDM: Factors affecting the quality of electrodes dressed on the machine”. Proceedings of IMechE, Part B, Volume 221, Number 3, pp 409-418, doi: 10.1243/09544054JEM645

[10] Whitesides. G.M (2006), The origins and the future of microfluidics. Nature 442, 368-373, doi:10.1038/nature05058

[11] B. Gehricke, I. Schruff, in: F. Jeglitsch (Ed.), Tool Steels in the Next Century: Proceeding of the Fifth International Conference on Tooling, 1999, pp. 83–90.

[12] C.A. Griffiths, S.S. Dimov, E.B. Brousseau, C. Chouquet, J. Gavillet, Investigation of surface treatment effects in micro-injection moulding, The International Journal of Advanced Manufacturing Technology. Volume 47, (1) (2009) 99–110. DOI 10.1007/s00170-009-2000-4

[13] E. Martinez, E. Engel, J.A. Planell, J. Samitier, Effects of artificial micro-and nano-structured surfaces on cell behaviour, Annals of Anatomy, Volume 191 (1) (2009), pages 126–135. doi:10.1016/j.aanat.2008.05.006

[14] A. Kovalchenko, O. Ajayi, A. Erdemir, G. Fenske, I. Etsion, The effect of laser surface texturing on transitions in lubrication regimes during unidirectional sliding contact, Tribology International, Volume 38, Issue (3), (2005), pages 219–225.

[15] A.S. Dimitrov, K. Nagayama, Continuous Convective Assembling of Fine Particles into Two-Dimensional Arrays on Solid Surfaces, Langmuir 12 (5) (1996), pages 1303–1311**.** DOI: 10.1021/la9502251

[16] A.A.G. Bruzzone, H.L. Costa, P.M. Lonardo, D.A. Lucca, Advances in engineered surfaces for functional performance, CIRP Annals Manufacturing Technology, Volume 57, Issue (2), (2008), pages 750–769, doi:10.1016/j.cirp.2008.09.003

[17] S.Y. Chou, P.R. Krauss, P.J. Renstrom, Imprint of sub-25 nm vias and trenches in polymers, Applied Physics Letters, Volume 67, Issue (21), (1995), pages 3114–3116, http://dx.doi.org/10.1063/1.114851

[18] W. Tillmann, E. Vogli, F. Hoffmann, Wear-resistant and low-friction diamond-like-carbon (DLC)-layers for industrial tribological applications under humid conditions, Surface and Coatings Technology, Volume 204, Issue (6–7), (2009) pages 1040–1045, doi:10.1016/j.surfcoat.2009.06.005

[19] A.A. Voevodin, C. Rebholz, A. Matthews, Comparative Tribology Studies of Hard Ceramic and Composite Metal-DLC Coatings in Sliding Friction Conditions, Tribology Transactions, Volume 38, Issue (4), (1995), pages 829–836, DOI:10.1080/10402009508983476

[20] B. Saha, E. Liu, S.B. Tor, D.E. Hardt, J.H. Chun, N.W. Khun, Improvement in lifetime and replication quality of Si micromold using N:DLC:Ni coatings for microfluidic devices, Sensors and Actuators B: Chemical, Volume 150, Issue (1) (2010), pages 174–182, doi:10.1016/j.snb.2010.07.019

[21] J. Robertson, Properties of diamond-like carbon, Surface and Coating Technology, Volume 50, Issue (3), (1992), pages 185–203, doi:10.1016/0257-8972(92)90001-Q

[22] A.A. Voevodin, M.S. Donley, J.S. Zabinski, Pulsed laser deposition of diamond-like carbon wear protective coatings: a review, Surface and Coating Technology Volume 92, Issue (1–2), (1997), pages 42–49, doi:10.1016/S0257-8972(97)00007-8

[23] J.A. Heimberg, K.J. Wahl, I.L. Singer, Superlow friction behavior of diamond-like carbon coatings: Time and speed effects, Applied Physics Letters, 78 (17) (2001) pages 2449–2451, doi: 10.1063/1.1366649

[24] B. Saha, E. Liu, S.B. Tor, N.W. Khun, D.E. Hardt, J.H. Chun, Replication performance of Si-N-DLC-coated Si micro-molds in micro-hot-embossing, Journal of micromechanics and microengineering, 20 (4) (2010) pages 1–8.

[25] F. Bremond, P. Fournier, F. Platon, Test temperature effect on the tribological behavior of DLC-coated 100C6-steel couples in dry friction, Wear, Volume 254, Issue (7–8), (2003), pages 774–783, doi:10.1016/S0043-1648(03)00263-1

[26] T. Sasaki, N. Koga, K. Shirai, Y. Kobayashi, A. Toyoshima, An experimental study on ejection forces of injection molding, Journal of Precision Engineering, Volume 24, Issue (3), (2000), pages 270–273, doi:10.1016/S0141-6359(99)00039-2

[27] Claudio V. Di Leo, Jacques Luk-Cyr, Haowen Liu, Kaspar Loeffel, New methodology for characterizing traction-separation relations for interfacial delamination of thermal barrier coatings, Acta Materialia, Volume 71, (2014), pages 306-318, doi:10.1016/j.actamat.2014.02.034

[28] Seokil Kang, Hyun-Pil Lim, Kwangmin Lee, Effects of TiCN interlayer on bonding characteristics and mechanical properties of DLC-coated Ti-6Al-4V ELI alloy, International Journal of Refractory Metals and Hard Materials**,** Volume 53, Part A, November 2015, Pages 13–16, doi:10.1016/j.ijrmhm.2015.04.028

[29] A.Escudeiro, M.A.Wimmer, T.Polcar, A.Cavaleiro. Tribological behaviour of uncoated and DLC-coated CoCr and Ti-alloys in contact with UHMWPE and PEEK counter bodies, Tribology International, Volume 89, (2015), pages 97-104, doi:10.1016/j.ijrmhm.2015.04.028, doi:10.1016/j.triboint.2015.02.002

[30] Zhang HL, Ong NS, Lam YC (2008) Experimental investigation of key parameters on the effects of cavity surface roughness in microinjection molding. Polymers Engineering & Science, Volume 48, Issue (3), pages 490–495, DOI: 10.1002/pen.20981

Highlights

A novel FEA approach to studying the DLC surface treatment of replication tools is studied.

FEA simulation modelling is utilised to identify the process temperature factors that lead to tool thermal expansion.

Dimensional changes that directly impact the life cycle of the coating are investigated.

Bulk temperature distributions are used to calculate the theoretical heat transfer influence on expansion.

Process optimisation can be used to reduce thermal expansion, thus reducing DLC coating delamination and cracking.

The micro injection moulding FEA shows unique frozen layer fraction results that identify rapid heat transfer to the DLC surfaces.